Journal of Fluorine Chemistry 132 (2011) 231–240

Contents lists available at ScienceDirect

Journal of Fluorine Chemistry

journal homepage: www.elsevier.com/locate/fluor

Review

Fluoride removal from water by chitosan derivatives and composites: A review

Patricia Miretzky [a,*], Alicia Fernandez Cirelli [b]

[a] Centro de Geociencias, Universidad Nacional Autónoma de México, Campus Juriquilla, Boulevard Juriquilla 3001, Queretaro 76230, Mexico
[b] Centro de Estudios Transdisciplinarios del Agua, Facultad de Ciencias Veterinarias, Universidad de Buenos Aires, Chorroarín 280, Buenos Aires 1427, Argentina

ARTICLE INFO

Article history:
Received 11 October 2010
Received in revised form 31 January 2011
Accepted 1 February 2011
Available online 1 March 2011

Keywords:
Fluoride removal
Chitosan derivatives
Chitosan composites
Rare earth metals

ABSTRACT

Fluoride is an essential element, indispensable for maintenance of dental health. Nevertheless, fluoride concentrations in drinking water above 1.5 mg L^{-1} may be detrimental to human health. Many methods have been developed for removing excessive fluoride from drinking water, adsorption seems to be an effective, environmentally friendly and economical one. Since the sorption capacity of fluoride below 2 mg L^{-1} on most conventional adsorbents is not satisfactory, much effort has been devoted to develop new and cost-effective fluoride adsorbents. This review reports the recent developments in the F^- removal in water treatment, using chitosan derivatives and composites in order to provide useful information about the different technologies. When possibly the adsorption capacity of chitosan derivatives and composites under different experimental conditions is reported to help to compare the efficacy of the fluoride removal process. A comparison with the adsorption capacity of other low cost adsorbents is also tabled.

Contents

1. Introduction

Fluoride is an essential element, indispensable for maintenance of dental health. Nevertheless, fluoride concentrations in drinking

* Corresponding author. Tel.: +52 442 2381104x132; fax: +52 442 2381100.
E-mail address: patovior@geociencias.unam.mx (P. Miretzky).

0022-1139/$ – see front matter © 2011 Elsevier B.V. All rights reserved.
doi:10.1016/j.jfluchem.2011.02.001

water above 1.5 mg L^{-1} may be detrimental to human health, leading to dental or skeletal fluorosis. The World Health Organization (WHO) has set a desirable and permissible limit range between 0.5 and 1.0 mg L^{-1} in drinking water [1].

Fluorosis is endemic in many parts of the world, particularly in mid latitude regions. Ground water with high fluoride concentrations occurs in large parts of Africa, China, the Middle East, southern Asia (India and Sri Lanka), United States, Mexico, Chile and Argentina [2–4]. Increasing amount of wastewater containing fluoride is being released from various engineering processes, such as semiconductor manufacturing, coal power plants, electroplating, rubber and fertilizer production, etc. [5].

Many methods have been developed for removing excessive fluoride from drinking water, such as the use of ion exchange columns, coagulation, use of membranes, electrochemical methods, but the high cost of these technologies makes them unpractical for developing countries. Excellent reviews of different technologies for the defluoridation of drinking water are those of Ayoob et al. [6] and Mohapatra et al. [7]. Among these techniques, adsorption seems to be an effective, environmentally friendly and economical one. Different adsorbents have been used for F removal, among them, activated alumina [8–10], titanium rich bauxite [11], synthetic resins [12], manganese oxide-coated alumina [13], carbon nanotubes [14,15], bone char [16], double layered hydroxides [17], kaolinite [18], etc. Activated alumina is the most common sorbent widely used for defluoridation of drinking water, but its optimal adsorption often works at low pH values, fact that increases dissolved aluminum in treated water [19]. Since the sorption capacity of fluoride on most conventional adsorbents is not satisfactory, and since a large number of materials that have been tested at relatively high fluoride concentrations displayed a very low capacity of fluoride removal below 2 mg L^{-1} [20], much effort has been devoted in recent years, to develop new and cost-effective fluoride adsorbents.

The use of adsorbents containing natural polymers has received great attention, in particular polysaccharides such as chitin and its derivate chitosan. Chitin is the second most abundant natural biopolymer after cellulose and the most abundant amino polysaccharide. It is found in the shells of crustaceans, shells and skeletons of mollusks and krill, on the exoskeletons of some arthropods and in the cell walls of some fungi [21,22].

Chitosan, a copolymer that is primarily composed of β (1→4) linked 2-amino-2-deoxy-D-glucopyranose units, and residual 2-acetamido-2-deoxy-D-glucopyranose units, is a chemical derivative obtained by alkaline deacetylation of chitin and also it is found naturally in some fungal cell walls. Since it is harmless to humans and presents excellent biological properties such as biodegradation in the human body, immunological, antibacterial, and wound-healing activity [23], chitosan has been widely used in food and pharmaceutical processes and in medical and agricultural drugs [24,25].

Chitosan is well known as an excellent biosorbent for metal cation removal in near-neutral solutions because the large number of NH_F groups. Excellent reviews on metal complexation by chitosan are those of Varma et al. [26], Crini [27] and Kurita [28]. Also, due to its cationic behavior, in acidic media, the protonation of amine groups leads to adsorption of metal anions by ion exchange [29–33].

Several methods have been used to modify natural chitosan either physically or chemically in order to improve the adsorption capacity. Chitosan naturally occurs in the form of flakes or powder which have limited utility particularly for column applications due to swelling, low mechanical strength, crumbling, etc. Attempts have been made to overcome these drawbacks through formation of chitosan beads through various routes [34].

Crosslinking with glutaraldehyde (GLA) or epichlorohydrin (ECH) can be cited as examples of chitosan chemical modifications. These reactions are done in order to prevent its dissolution in acidic solutions or to improve metal sorption properties (to increase sorption capacity and/or to enhance sorption selectivity) [35]. It must be taken into account that crosslinking can reduce the adsorption capacity as it diminishes the quantities of free amino groups, but this loss of capacity may be necessary to ensure stability of the polymer. The adsorption capacity of chitosan varies with porosity, crystallinity, affinity for water, percent deacetylation and the related amino group content [36].

Chitosan can be molded in several shapes, membranes, microspheres, gel beads, films, nanoparticles and nanofibers [37–39], and is able to provide a ratio: surface area/mass that maximizes the adsorption capacity and minimizes the hydrodynamic limitation effects, such as column clogging and friction loss [40]. Due to these facts, some authors have studied several ways to support chitin and chitosan by means of synthetic materials such as polymers. Polymeric supports have advantages such as easy handling and versatility. Also it is possible to obtain homogeneous, porous, malleable and mechanically–chemically resistant biocomposites. However, at the same time, their sorption capacity is reduced due to blockage of adsorption sites by the physical and chemical interactions between the supporting media and the biopolymer [41]. Different mineral materials as hydroxyapatite, binary metal oxides, magnesia, hydrotalcite, alumina, rare earth metals, etc. have been supported on chitosan resulting in inorganic composites with high F removal capacity [42–56] etc.

The aim of this study is to review the literature in order to provide useful information about the different technologies for F removal from solution using chitosan and its derivatives and when possibly to report the adsorption capacity under different experimental conditions.

2. Physicochemical characteristics of chitosan

Chitosan, poly-β(1-4)-2-amino-2-deoxy-D-glucopyranose is a polysaccharide obtained by partial or total N-deacetylation of chitin poly-β(1-4)-2-acetamide-2-deoxy-D-glucopyranose. The difference between chitin and chitosan is the deacetylation degree and their respective solubility in dilute acidic media. Chitosan is the only derivative soluble at a degree of deacetylation above 40% [57]. Although the polymer backbone consists of hydrophilic functional groups, chitosan is normally insoluble in water at near neutral pH and most common organic solvents (e.g. DMSO, DMF, NMP, organic alcohols, pyridine). The insolubility of chitosan in aqueous and organic solvents is a result of its crystalline structure, which is attributed to extensive intramolecular and intermolecular hydrogen bonding between the chains and sheets, respectively [58].

The degree of deacetylation depends on the raw material from which chitin was obtained and the experimental procedure, and controls the fraction of free amino groups that will be available for interactions with metals ions [35]. When the degree of deacetylation of chitin is larger than 40–50%, chitosan becomes soluble in acidic media. The solubilization occurs by protonation of the NH_2 groups on the C2 position of the D-glucosamine unit, although the distribution of acetyl groups along the chain may modify solubility [59]. The presence of amino groups makes chitosan a cationic polyelectrolyte (pK_a = 6.5), one of the few found in nature.

Chitosan can be modified by chemical or physical processes in order to improve the mechanical and chemical properties. The efficiency of adsorption depends on physicochemical properties, mainly surface area, porosity and particle size of adsorbents. Chitosan has a very low specific area ranging between 2 and 30 $m^2 g^{-1}$ whereas most commercial activated carbons range

between 800 and 1500 $m^2 g^{-1}$ [27]. Chitosan based material are used in different fields of application in the form of powder, flakes and foremost as gels: beads, membranes, sponge, fibers, hollow fibers, etc. [60,61]. Flake and power forms of chitosan are not suitable to be used as adsorbents due to their low surface area and no porosity [26]. Chitosan flakes modified into beads are essential for the enhancement of adsorption performance [35]. There are many studies describing the preparation of chitosan gels [62,63].

The chemical modification of chitosan is of special interest when this modification does not change the fundamental skeleton of chitosan but brings new or improved properties. A great number of chitosan derivatives have been obtained by grafting new functional groups on the chitosan backbone to increase the metal adsorption capacity. The new functional groups are incorporated to increase the density of sorption sites, to change the pH range for metal sorption and to change the sorption sites in order to increase sorption selectivity for the target metal [28]. The chemical modification affords a wide range of derivatives with modified properties for specific use and applications in diversified areas mainly of pharmaceutical, biomedical and biotechnological fields [64].

Cross linking agents are generally composed by functional groups separated by some spaced molecules that can be structured in various forms (rings, straight chains, branched chains). The crosslinking agents can be of varying length and contain other functional groups than those involved in cross linking. Partial crosslinking by di/polyfunctional reagents enables the use of chitosan for metal adsorption in acidic medium. In a general way, the adsorption capacity decreases with the extent of crosslinking as it diminishes the reactive sites on the chitosan polymer but also, it can improve the adsorption capacity, depending on the functional groups in the crosslinking agent [65], being the most common, glutaraldehyde (GLA), ethylene glycol diglycidyl ether (EGDE) and epichlorohydrin (EPI).

3. Characterization of chitosan and chitosan derivatives

The identification of chitosan and chitosan derivatives has been carried out by different non destructive techniques (Table 1): X-ray diffraction (XRD) [46,48,49,66], scanning electron microscopy coupled with energy dispersive X-ray spectroscopy (SEM–EDX) [47,66–69], Fourier transform infrared spectroscopy (FTIR) [44,45,48,49,70]. Excellent reviews on description and discussion of the different techniques mentioned above can be seen elsewhere [71–73].

4. Fluoride detection

Fluoride analysis has been carried out by the fluoride selective electrode method (ASTM D1179-B). TISAB (III) solution was used as a buffer for maintaining the pH and background ion concentrations [43–56,66–70,74,75]. Also fluoride concentration determination was carried on using zirconyl-SPADNS dye and UV–Vis spectrophotometer (EPA 340.1 method) by Kamble et al. [42].

5. Fluoride sorption studies

5.1. Chitosan and chitosan modified materials

Results on F^- adsorption onto chitosan and chitosan derivatives from different researchers are shown in Table 1.

Defluoridation studies on natural chitosan were performed by Menkouchi Sahli et al. [76]. Batch experiments were carried out under different experimental conditions. The adsorption data were fitted to Langmuir and Freundlich isotherms. The maximum adsorption capacity reported was 1.39 mg g^{-1}.

Carboxylated cross-linked chitosan beads (CCB) were investigated as F^- adsorbent material [67]. The chitosan beads were crosslinked with glutaraldehyde. In order to effectively utilize the hydroxyl groups of chitosan and in this way enhance the defluoridation capacity, the carboxylic group was introduced using chloroacetic acid. Batch experiments were performed under different experimental condition to investigate the F^- removal capacity of CCB. The defluoridation capacity was not influenced by the pH of the medium and slightly affected in the presence of co-anions. Adsorption data were fitted to Langmuir and Freundlich isotherms. The maximum adsorption capacity was 11.11 mg g^{-1}. The nature of the F^- adsorption process was spontaneous and endothermic. The rate of F^- adsorption reaction followed pseudo second order kinetic and intraparticle diffusion models. The mechanism proposed was H-bonding between acidic hydrogen (–COOH) and the fluoride ions.

The defluoridation capacity of protonated cross linked chitosan beads was investigated [65]. This study was carried out in a similar way to the one mentioned before. The maximum adsorption capacity was 7.32 mg g^{-1}(303 K). The adsorption process was spontaneous and endothermic. The rate of reaction followed non linear pseudo-second order and intra-particle diffusion kinetic models. The sorption mechanism suggested was H-bonding between protonated amine groups ($NH3^+$) and F^- ions. Viswanathan et al. [69] also studied the defluoridation capacity of chemically modified chitosan beads by introducing $NH3^+$ and COOH groups by means of chitosan protonation and carboxylation.

5.2. Electropositive multivalent metals incorporated to chitosan beads

Fluoride ion is classified as a hard base due to its high electronegativity and small ionic size and presents strong affinity for electropositive multivalent metal ions like transition and rare earth metals (Al (III), Fe (III), Ti (IV), La (III), Zr (IV), Ce (III), etc. As rare earth metals are expensive, a number of researchers have loaded these metals on cheaper components as chitosan supports to enhance adsorption capacity and to diminish the adsorbent cost.

It is a well known fact that the N in the NH_2 group of chitosan acts as an electron donor and it is responsible for selective chelation with metal ions (La^{3+}, Ce^{4+}, Fe^{3+}, Ti^{4+}, Al^{3+}, etc.) [50,51]. These metal ions complete heir coordination shells with OH groups, that can bind or release H^+ depending on the solution pH. Under acidic conditions, the OH groups are protonated and can adsorb F^- ions through exchange mechanism. At acid pH, the fluoride sorption capacity is diminished probably due to formation of HF and at alkaline pH values, fluoride sorption also is lower due to competition with OH^- ions.

Results on F^- adsorption onto chitosan composites from different researchers are shown in Table 1.

5.2.1. Mg

Magnesia (MgO) is a well known adsorbent with high defluoridation capacity. In order to overcome the limitations of MgO for field application, Sundaram et al. [45] used a composite magnesia/chitosan (MgOC) for F^- removal from aqueous solution. Equilibrium data fitted Langmuir and Freundlich isotherm, the maximum adsorption capacity for F^- removal was 11.24 mg g^{-1} (303 K). Evaluation of the thermodynamic parameters suggested the spontaneous and endothermic nature of the adsorption process. The kinetics of F^- adsorption onto MgOC followed pseudo-second order model and particle and intraparticle diffusion models. The adsorption mechanism suggested was ion exchange. Since the pH_{zpc} of MgOC is 10.6, the adsorbent was positively charged up to this pH value; hence the adsorbent was able to remove F^- ions by electrostatic attraction for a wide pH range. Also, chitosan could also contribute to the F^- adsorption capacity by removing F^- ions through hydrogen bonding.

Table 1
Fluoride adsorption by chitosan derivatives and composites.

Adsorbent material	Q_{max} ($mg\,g^{-1}$)	pH optimal	Type of study	Isotherm	Kinetic model	Thermo-dynamics	Mechanism proposed	Adsorbent characterization	Reference
Chitosan and chitosan derivatives									
Chitosan	1.39	6.0	E	L, F					[76]
Carboxylated crosslinked chitosan beads	11.11	7.0	E, K, T	L, F	Pseudo second order, intraparticle diffusion	Spontaneous, endothermic	Electrostatic adsorption and Lewis acid–base interaction	SEM, EDX, FTIR	[67]
Protonated cross-linked chitosan beads	7.32	7.0	E, K, T	L, F	Pseudo second order, intraparticle diffusion	Spontaneous, endothermic	Electrostatic adsorption	SEM, EDX, FTIR	[68]
Multifunctional cross-linked chitosan beads	6.25	7.0	E, K, T	L, F	Non linear pseudo second order, intraparticle diffusion	Spontaneous, endothermic	Electrostatic adsorption	SEM, EDX, FTIR	[69]
Mg–chitosan									
Magnesia–chitosan composite	11.24	3.0–11.0	E, K, T	L, F	Pseudo second order, particle and intraparticle diffusion model	Spontaneous, endothermic	Electrostatic attraction; H bonding	FTIR	[45]
Al–chitosan									
Al impregnated chitosan biopolymer	1.7316	6.5	E, K, T	L, F	Lagergren first order	Spontaneous, endothermic	Electrostatic attraction	SEM, EDX	[47]
Alumina/chitosan composite	10.417	7.0	E, K, T	L, F	pseudo second order, particle and intraparticle diffusion	Spontaneous, endothermic	Electrostatic adsorption, complexation	SEM, EDX, FTIR	[56]
Fe–chitosan									
Fe (III) carboxylated chitosan beads	15.385	7.0	E, K, T	L, F	Pseudo second order, intraparticle diffusion	Spontaneous, endothermic	Electrostatic adsorption, complexation	SEM, FTIR	[50]
Ti–chitosan									
Ti–chitosan spherical beads	7.2	7.0	E, K, T	L, F	Lagergren, intraparticle diffusion model	Spontaneous, endothermic	Anion exchange between Ti–OH and F	XRD, SEM, FTIR, BET	[47]
Ti–Al chitosan									
Ti–Al binary metal oxide supported chitosan beads	2.22	3.0–9.0	E, K, T	L, F	Pseudo second order, intra-particle diffusion model	Spontaneous, exothermic	Electrostatic attraction	SEM, XRD, FTIR	[49]
SiO_2–chitosan									
Chitosan coated silica	44.4	4	E, D, K	L, F	Pseudo second order		Ion exchange	SEM, XRD, FTIR, TGA	[74]
La–chitosan									
La (III) carboxylated chitosan beads	11.905	7.0	E, K, T	L, F	Pseudo second order, particle and intraparticle diffusion	Spontaneous, endothermic	Electrostatic adsorption, complexation	SEM, EDX, FTIR	[51]
La–chitosan beads	4.7	5.0	E, K, T	L, F	Lagergren, inter and intraparticle diffusion model	Spontaneous, endothermic	Anion exchange between La–OH and F	XRD, SEM, EDX, FTIR, BET	[42,66]
La–chitosan beads	4.7		E	L, F			Electrostatic attraction	XRD	[48]
Zr–chitosan									
Zr (IV) entrapped chitosan polymeric matrix	13.699	7.0	E, T	L, F, D–R		Spontaneous, endothermic	Electrostatic adsorption and complexation	SEM, EDX, FTIR	[52]
Chitosan supported Zr (IV) tunsgtophosphate composite	7.634	3.0	E, K, T	L, F	Pseudo second order, intraparticle diffusion	Spontaneous, endothermic	Adsorption, complexation, ion exchange	SEM, EDX, FTIR	[54]
Ce–chitosan									
Ce (III) encapsulated chitosan polymeric matrix	9.00	7.0	E, T	L, F	Pseudo second order, intraparticle diffusion	Spontaneous, endothermic	Electrostatic adsorption and complexation	SEM, EDX, FTIR	[53]
Nd–chitosan									
Neodymium–modified chitosan	11.41	7.0	E, K	L, F	Pseudo second order, boundary layer and intraparticle diffusion		Ion exchange	FTIR	[75]

Table 1 (*Continued*)

Adsorbent material	Q_{max} (mg g^{-1})	pH optimal	Type of study	Isotherm	Kinetic model	Thermo-dynamics	Mechanism proposed	Adsorbent characterization	Reference
Chitosan-composites									
Nano hydroxyapatite–chitosan composite	2.04	3.0	E, K, T	L, F	Pseudo second order, pore diffusion model	Spontaneous, endothermic	Chemisorptions and ion exchange		[43]
Nano hydroxyapatite–chitin composite	8.41	3.0	E, K, T	L, F	Pseudo second order, pore diffusion model	Spontaneous, endothermic	Chemisorptions and ion exchange	SEM, EDX, FTIR	[44]
Chitin-biocomposite		5.0							[41]
Hydrotalcite/chitosan composite	1.876	3.0	E, K, T	L, F	Pseudo second order, intraparticle diffusion	Spontaneous, endothermic	Ion exchange	SEM, EDX, FTIR	[55]
Magnetic chitosan									
Magnetic chitosan particles	20.96–23.98	7.0	E, K	L, 2-sites L, B, F, D–R	Pseudo second order		Physical (Van der Waals)	SEM, XRD, FTIR	[70]

E; equilibrium; K: kinetic; D: dynamic; T: thermodynamic; L: Langmuir; F: Freundlich; D–R: Dubinin–Radushkevich; B: Brunauer isotherms; X-ray diffraction (XRD); scanning electron microscopy (SEM); scanning electron microscopy coupled with energy dispersive X-ray spectroscopy (SEM–EDX); Fourier transform infrared spectroscopy (FT-IR), thermogravimetric analysis (TGA).

5.2.2. Al

Aluminum impregnated chitosan (AIC) was prepared and applied as an adsorbent for the removal of F^- ions form aqueous solution [47]. Batch adsorption experiments on AIC were carried out at different pH, contact time, dose, presence of diverse anions and initial fluoride concentration to determine the optimum adsorption conditions. Experimental data were fitted to Langmuir and Freundlich isotherms. The maximum adsorption capacity for F^- ions onto AIC was 1.73 mg g^{-1}. The adsorption process followed first order Lagergren model kinetics. Thermodynamic parameters suggested that the adsorption process was spontaneous and endothermic in nature. At low pH values, the surface of the adsorbent was positively charged and F^- was removed by exchange process. The AIC adsorbent could be regenerated at pH 12.

In order to improve the adsorption capacity of alumina, alumina/chitosan composite (AlCs) was prepared by incorporating alumina particles in the chitosan polymeric matrix [56]. The effect of different experimental parameters was studied and adsorption equilibrium data were fitted to Langmuir and Freundlich isotherms. The maximum F^- adsorption capacity was 10.42 mg g^{-1}. Thermodynamic parameters suggested that the adsorption process was spontaneous and endothermic in nature. Kinetic studies determined that the process followed pseudo-second order and particle and intraparticle diffusion models. The fluoride removal by AlCs composite was mainly governed by electrostatic adsorption and complexation mechanisms.

5.2.3. Fe

Fluoride removal by Fe (III) loaded carboxylated chitosan beads (Fe–CCB) was investigated [50]. Batch experiments were carried on under different experimental conditions, pH, contact time, initial fluoride concentration, adsorbent dose, presence of competitor co-anions, etc. Experimental data were fitted to Langmuir and Freundlich isotherms. The fluoride maximum adsorption capacity was 15.38 mg g^{-1} (303 K). Thermodynamic parameters suggested the spontaneous and endothermic nature of the adsorption process. Kinetic studies were carried on with reaction-based and diffusion based models. The pseudo second order model and the intraparticle model were the best fit for experimental data. The main sorption mechanism proposed was complexation through chitosan–NH_2 groups chelated with Fe^{3+} ions and electrostatic attraction between chitosan–COO–Fe^{3+} groups and fluoride ions, whereas with carboxylated chitosan beads, the adsorption mechanism was only H-bonding between HCOO–chitosan groups and fluoride ion.

5.2.4. Ti

The metal binding property of chitosan was used to incorporate Ti metal and applied as an adsorbent for fluoride removal [47]. The influence of different experimental parameters such as pH, initial F^- concentration, adsorbent dose, and presence of coexisting anions was investigated. Experimental data were fitted to Langmuir and Freundlich isotherms. The maximum adsorption capacity was 7.21 mg g^{-1}. Thermodynamic parameters indicated that the adsorption process was spontaneous and endothermic. The authors concluded that the mechanism of adsorption of fluoride was complex and that surface adsorption and also intra-particle diffusion contributed to the rate determining step. The adsorption mechanism was ionic exchange between OH^- from chitosan–Ti–OH groups (Ti (IV) coordinated with chitosan through NH_2 groups) and F^- ions.

5.2.5. Ti–Al

The performance of Ti–Al binary metal oxide supported beads using chitosan template was studied for fluoride removal from

drinking water [49]. The higher removal capacity of the synthesized adsorbent (Q_{max} = 2.22 mg g^{-1}) compared to bare chitosan was due to higher surface area. The effect of different experimental parameters on F^- adsorption on the adsorbent was investigated. The experimental data were fitted to Langmuir and Freundlich adsorption models and to pseudo-second order and intra-particle diffusion kinetic models. The adsorption process was spontaneous and exothermic in nature. It was observed that multiple treatments with 2% alum ($KAl(SO_4)_2{\cdot}12H_2O$) solution regenerated 80% of the adsorbent. The effect of flow rate on fluoride adsorption capacity was also studied in column experiments.

5.2.6. SiO_2

Chitosan coated silica (CCS) was used for defluoridation of aqueous solution [74]. The effect of experimental parameters such as pH, contact time, adsorbent dose and initial fluoride concentration was investigated through batch experiments. Adsorption data were fitted to Langmuir and Freundlich isotherms. The maximum adsorption capacity was 44.4 mg g^{-1}. The kinetic studies indicated that F^- sorption onto CCS followed pseudo-second order kinetics.

5.2.7. La

Kamble et al. [42] investigated the effects of different parameters (pH, adsorbent dose, initial F^- concentration, the presence of interfering ions) on the adsorption of F^- by chitin, chitosan and chemically modified La–chitosan (20% of La loading). The authors concluded that the F^- removal capacity and affinity of 20% La–chitosan was higher than that of chitin and chitosan. The presence of anions, particularly carbonate and bicarbonate diminished F^- adsorption. Experimental adsorption data fitted Freundlich isotherm and Lagergren first-order model. It was concluded that the mechanism of F^- removal by 20% La–chitosan was complex and both the surface adsorption and the intra-particle diffusion contributed to the rate determining step.

Viswanathan and Meenakshi [51] investigated the defluoridation capacity of La–carboxylated chitosan beads (La–CCB). The adsorption experimental data were fitted to Langmuir and Freundlich isotherms. The authors reported that the maximum F^- adsorption capacity of La–CCB was 11.905 mg g^{-1} (303 K) almost 3 times higher than the one of carboxylated chitosan beads. Thermodynamic parameters suggested the spontaneous and endothermic nature of the adsorption process. The kinetic studies were carried on with reaction-based and diffusion based models. The pseudo second order model and both the particle and intraparticle model were the best fit for experimental data. The authors suggested that La–CCB removed F^- ions by complexation through NH_2 chitosan groups chelated with La^{3+} ions. In addition there is a possibility of exchange of La^{3+} ion for H^+ ion in carboxyl group of chitosan, which contains oxygen atom acting as an electron pair donor to the Lewis acid (La^{3+}) followed by electrostatic attraction between chitosan–COO–La^{3+} groups and fluoride ions.

Synthesis of lanthanum incorporated chitosan beads (LCB) and its application for the removal of F^- ions from groundwater was also investigated by Bansiwal et al. [66] and Thakre et al. [48]. The synthesis was optimized by varying different parameters such as lanthanum loading, complexation and precipitation time, concentration of ammonia solution used for precipitation, etc. The effect on the adsorption capacity of pH, adsorbent dose, initial F^- concentration, presence of other anions and cations was investigated. La–chitosan beads showed fluoride removal efficiency of 97% at pH 5. The presence of other anions affected the fluoride uptake. The maximum adsorption capacity was 4.7 mg g^{-1}. Adsorption data fitted Langmuir isotherm. The kinetics of the adsorption process was rapid and data followed pseudo-first order kinetics. The authors concluded that the adsorption of fluoride process was complex and involved surface adsorption and also inter and intra-particle diffusion. Thermodynamic parameters suggested that the adsorption process was spontaneous and endothermic. The fluoride loaded material could be regenerated after complete saturation with NH_4Cl 1 M (81.22% regeneration capacity).

5.2.8. Zr

Zr (IV) loaded carboxylated chitosan beads (Zr–CCB) were synthesized and fluoride removal studies were carried out in batch experiments under different experimental conditions [52]. The effect of pH, contact time, initial fluoride concentration, competitor anions, was investigated. The adsorption data were fitted to Langmuir, Freundlich and Dubinin–Radushkevich (D–R) isotherms. The maximum adsorption capacity was 13.699 mg g^{-1} (303 K). The fluoride adsorption process was spontaneous and endothermic as ΔG° and ΔH° values were negative and positive respectively. No kinetic studies were reported. The mechanism proposed was similar to that proposed for La–CBB mentioned before.

A new biocomposite was prepared by incorporating Zr (IV) tungstophosphate, an inorganic ion exchanger into chitosan biopolymeric matrix [54]. The adsorption of F^- ions on this biocomposite was investigated by batch technique. The influence of pH, contact time, initial F^- concentration, competing co-ions and temperature in the adsorption process was investigated. The equilibrium adsorption data were fitted to Langmuir and Freundlich isotherms, the maximum adsorption capacity was 7.63 mg g^{-1}. The kinetics of the adsorption process followed pseudo-second order and intra-particle diffusion models. The thermodynamic parameters suggested the spontaneous and endothermic nature of the F^- adsorption.

5.2.9. Ce

Chitosan modified by carboxylation followed by chelation with Ce (III) was investigated as and adsorbent for F^- removal from aqueous solution [53]. Experimental batch studies were conducted under different pH, contact time, presence of competitor co-anions. The experimental data were fitted to Freundlich and Langmuir isotherms. The maximum adsorption capacity was 9.00 mg g^{-1}. Thermodynamic parameters confirmed the spontaneous and endothermic nature of the adsorption process. The kinetic data were fitted to reaction and diffusion based models. The pseudo-second order and intra-particle diffusion models were the more significant in defining the fluoride sorption process. The mechanism proposed was similar to that for La–CCB mentioned before.

5.2.10. Nd

The applicability of neodymium–modified chitosan as F^- adsorbent from aqueous solution was studied [75]. The effect of temperature, adsorbent dose, particle size and the presence of co-ions on the adsorption process was investigated. The experimental data were fitted to Langmuir and Freundlich isotherms. The maximum adsorption capacity was 11.41 mg g^{-1} (283 K). Sorption studies revealed that the pseudo-second order was suitable to describe the F^- adsorption process onto the adsorbent. The process was complex, and both the boundary of liquid film and intra-particle diffusion contributed to the rate determining step. The adsorbent was regenerated in 24 h by a 4 g L^{-1} NaOH solution.

5.3. Chitosan biocomposites

The development of polymeric composite materials in which the combination of the properties of the constituents lead to an increase of the functional or structural properties of the composite

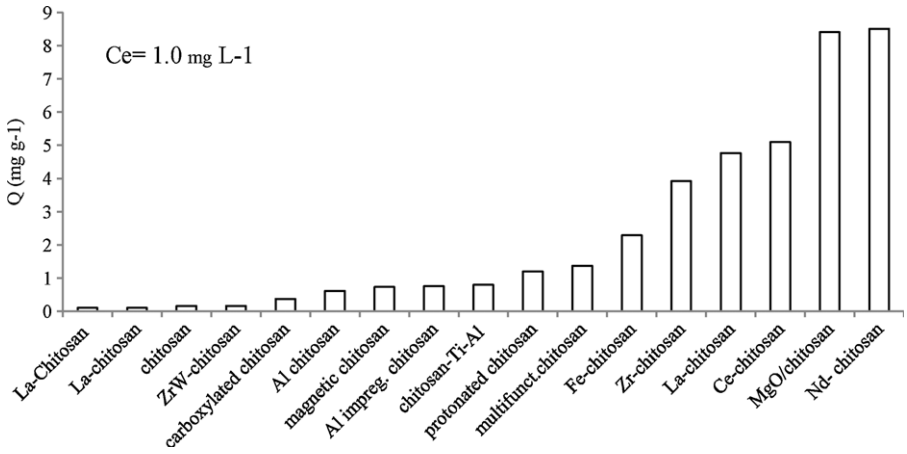

Fig. 1. Fluoride removal capacity by different chitosan derivatives and composites (C_e = 1.0 mg L^{-1}).

material is of great interest. The composites based on biodegradable materials have received more attention because they are environmentally friendly.

Nano hydroxyapatite (n-HAp) was found to have high defluoridation capacity (Q_{max} = 3.113 mg g^{-1}) and also low cost and availability [77]. However when n-Hap powder has been used as such, it causes significant pressure drop during filtration and this disadvantage out weights its advantage of higher F^- removal. In order to overcome this problem, n-Hap was made into a biocompatible biocomposite with chitosan which could be made into any desirable form [43]. Batch experiments were carried on to study the influence of different experimental parameters on the F^- adsorption by the composite material. Data were fitted to Langmuir and Freundlich isotherms; the maximum adsorption capacity was 2.040 mg g^{-1} (30 °C). The adsorption process was spontaneous and endothermic. The rate of sorption followed pseudo-second order kinetic model and occurred through pore diffusion. The main mechanism responsible for F^- adsorption onto the biocomposite material was electrostatic attraction between the positive surface and negatively charged fluoride ions. Similar studies were carried on using nano-hydroxyapatite/chitin composite [44]. The maximum adsorption capacity was 8.41 mg g^{-1} higher than that of n-HAp/chitosan. The authors suggested that the enhancement of the defluoridation capacity with respect to n-Hap might be due to biosorption by chitin, adsorption by physical forces and fluoride ion entrapped in fibrilliar capillaries and spaces of polysaccharide network of the chitin moiety, but they did not explain the different defluoridation capacity between chitosan a chitin biocomposites.

The optimum composition of a chitin based biocomposite was determined based on both its fluoride adsorption capacity and it is chemical resistance in acid aqueous solution [41]. Chitin content, polyurethane polymer content, catalyst content, chitin particles size, degree of acetylation of chitin and effect of pH on the F^- adsorption was investigated. No isotherm or kinetic studies were carried on. The optimized biocomposite adsorbed 0.29 mg g^{-1} at F^- initial concentration of 15 mg L^{-1} and pH 5.0.

The hydrotalcite (HT) adsorption capacity was enhanced by preparation of HT/chitosan composite [55]. Hydrotalcite is a layered doubled hydroxide with a general formula $[M^{2+}_{1-x}\,M^{3+}_{x}(OH)_2]^{x+}\,[A^{n-}_{x/n}\cdot m_2O]^{x-}$ where M^{2+} and M^{3+} are di- and trivalent metal cations and A is an interlamellar anion with charge n^-. Fluoride adsorption experiments were carried on under different experimental conditions. Experimental data were fitted to Langmuir and Freundlich isotherms. The fluoride maximum adsorption capacity was 1.876 mg g^{-1} (30 °C) and increased with temperature. The F^- removal process was spontaneous and endothermic. Adsorption data were best fitted to pseudo-second order and intra-particle diffusion kinetic models. The adsorption mechanism suggested was ion exchange between counter ions at positive surface sites on HT and chitosan, and also the exchange of

Table 2
Fluoride maximum adsorption capacity on different materials.

Adsorbent material	Q_{max} (mg g^{-1})	Reference
Quartz	0.19	[20]
MnO_2 coated activated alumina	0.17	[80]
Activated and MnO_2 coated tamarind fruit	0.22	[81]
Plaster of Paris	0.34	[82]
Calcite	0.39	[20]
Activated alumina	0.74	[8]
Laterite	0.85	[83]
Activated alumina	1.08	[13]
Fe activated quartz	1.16	[20]
Synthetic siderite	1.77	[84]
Fluorspar	1.79	[20]
Al-impregnated C	1.80	[85]
Mg bentonite clay	2.26	[86]
Alfa alumina	2.73	[87]
Aligned C nanotubes	2.85	[14]
MnO_2 coated alumina	2.85	[13]
La-impregnated silica gel	3.80	[88]
Ti rich bauxite	3.80	[11]
10% La–bentonite	4.24	[89]
Carbon slurry	4.31	[90]
Hydroxyapatite	4.59	[20]
Alum sludge	5.39	[91]
Activated red mud	6.29	[92]
γ alumina	6.36	[5]
Polyacrilamyde Ce (IV)–PO_4 resin exchanger	7.75	[93]
Polyacrilamyde Zr (IV)–PO_4 resin exchanger	8.55	[93]
Alumina cement granules	10.22	[78]
Polyacrilamyde Al (III)–PO_4 resin exchanger	10.87	[93]
Bone char	11.90	[16]
Activated alumina	12.10	[88]
Mixed rare earth oxides	12.50	[94]
Mesoporous alumina	14.26	[5]
Hydrous ferric oxide (HFO)	16.50	[79]
Activated Ca–charcoal (650 °C)	19.05	[95]
La-impregnated crosslinked gelatin	21.28	[96]
Amorphous alumina supported on C nanotubes	24.15	[97]
Zr (IV) impregnated collagen fiber	41.42	[98]
La-exchanged zeolite F-10	45.15	[99]
Al–Ce hybrid adsorbent	91.40	[19]
Ce (IV) oxide/SiMCM-41	114.40	[100]
Fe–Al Ce trioxide	195.0	[101]
MgAl–CO_3 layered double hydroxides	319.80	[17]

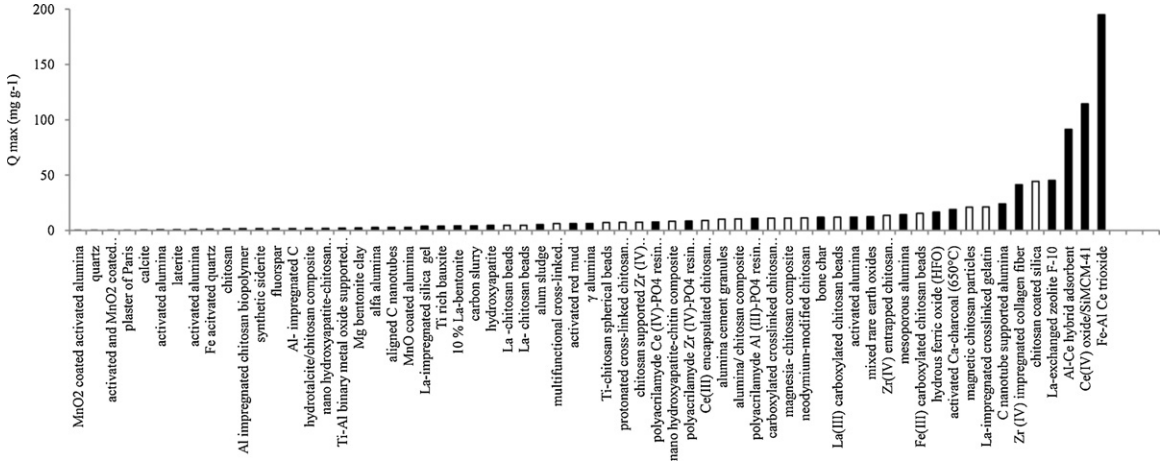

Fig. 2. Comparison of maximum adsorption capacity of different fluoride adsorbents.

interlayer anions of HT and structural hydroxyl groups of the HT layers.

5.4. Magnetic chitosan particle

A magnetic chitosan particle was prepared by the co-precipitation method with Fe^{2+} and Fe^{3+} solutions (ratio Fe^{3+}/Fe^{2+} = 3:2), and employed to remove F^- ions from water solution [70]. The two sites Langmuir isotherm and Bradley's equation were fitted well with the experimental adsorption data. Maximum adsorption capacity reported was 22.49 mg g^{-1}. Results from Dubinin–Radushkevich (D–R) isotherm suggested that the adsorption was physical as E_a was 2.48 kJ mol^{-1}. Adsorption data fitted pseudo-second order kinetic model. The authors suggested that the principal adsorption mechanism was F^- physical interaction with the NH_2 and Fe–O groups on the surface of the magnetic particle.

5.5. Comparison of sorbent effectiveness of chitosan derivatives and composites

It has to be mentioned that the F^- maximum adsorption capacity of different adsorbents reported in Table 1 gives us some idea of sorbent effectiveness, as it depends on experimental conditions (pH, temperature, dose, ionic strength, particle size, presence of competing ions etc.). Generally the adsorption capacity of an adsorbent increases with increasing F^- initial concentration until saturation conditions. The isotherm studies performed for a higher range of fluoride concentrations will show higher capacity than those of lower ranges and the maximum adsorption capacity obtained from Langmuir isotherm will differ in both cases [78], so it is important to take into consideration the initial fluoride concentration range, when performing comparative studies. Fluoride concentration in ground waters of the worst affected countries like India are in the range of 0.5–48 mg L^{-1}. Nonetheless, it is not uncommon to encounter isotherm studies performed at fluoride concentration of 1000 mg L^{-1} [79] and even up to 2500 mg L^{-1}[17].

In most of the papers reviewed the isotherm studies are carried on by varying the initial concentration of the F^- solution. But in groundwater, the F^- concentration remains constant, so it seems more representative of natural waters to run isotherm studies on dose-variation of adsorbents instead of studies on fluoride concentration variation [78].

It has to be taken into account that some of the adsorbents reported presented high adsorption capacity at high F^- equilibrium concentration in water, but, in water treatment, the final concentration of F^- in the water solution must be below 1.0 mg L^{-1}. So it is desirable that the adsorbent presents high adsorption capacity at low fluoride equilibrium concentrations. The F^- adsorption capacity corresponding to F equilibrium concentration 1.0 mg L^{-1} is seldom reported, but can be calculated from isotherm equations. As seen in Fig. 1, the best F^- adsorbents reviewed in this paper were Nd–chitosan and MgO–chitosan followed by rare earth metal–chitosan derivatives because they presented higher adsorption capacity at the equilibrium F^- concentration of 1 mg L^{-1}.

6. Comparison between chitosan and other low cost adsorbents performance

A research of the recent literature has already been conducted on fluoride sorption by a wide variety of low cost adsorbents. Results on the fluoride sorption performance by alumina and alumina based materials, clays and soils, calcium based minerals, metal oxides, carbon based materials and synthetic materials are listed in Table 2.

Although as noted before, the maximum adsorption capacity is reported in this paper only to give some idea of sorbent effectiveness, a comparison between results reported in Tables 1–2 shows that chitosan derivatives, mainly at the right extreme of Fig. 2, present good F^- removal capacities, only surpassed by Al–Ce hybrid, Ce (IV) oxide/SiMCM and Fe–Al–Ce trioxide. We have already mentioned that rare earth metals have strong affinity to fluoride. As they are very expensive, usually they are mixed with cheaper materials to reduce costs and maintain the high fluoride adsorption capacity. In the case of the Al–Ce hybrid adsorbent, the pH_{ZCP} 9.6 results in fluoride adsorption on the positive adsorbent via electrostatic interaction. The hydrated cerium (IV) oxide on the surface of SiMCM-41 has a high affinity for the fluoride ion, being the adsorption mechanism anion exchange between the hydroxyl groups existing on the surface of (Ce)SiMCM-41 and F^- ions. In the trioxide, the aluminum oxide which has a pH_{ZPC} near 8.0 contributes to a high performance.

Many times, chemically modification of different materials increases the adsorption capacity, but the technology cost must be taken in consideration in order to produce real "low-cost" adsorbents.

7. Conclusions

Performance comparison of different low-cost adsorbents is difficult because of inconsistencies in data, principally due to different experimental conditions (pH, temperature, ionic

strength, particle size, range of initial fluoride concentration, presence of competing ions, etc.). Cost information is seldom reported in the publications because it depends on local availability and on the technology applied.

In this paper, a recent literature review of F^- adsorption by chitosan and by chemical modified chitosan is presented. In a great number of papers reviewed the experimental data of the F^- adsorption process have been fitted to Langmuir or to Freundlich models. Regeneration and reusing of the chitosan derivatives and composites is reported when it is possible. Chitosan derivatives and composites present fluoride maximum adsorption capacity ranging from 1.39 mg g^{-1} for raw chitosan [76] to 44.4 mg g^{-1} for chitosan coated silica [74]. The effect of competitive anions, in particular carbonate and bicarbonate ions, is an important issue that needs to be more studied as they decrease the fluoride adsorption capacity of chitosan derivatives.

The use of chitosan composites and derivatives for removing F^- ions from contaminated solutions presents many attractive features such as the high adsorption capacity and the fact that chitosan is obtained from natural raw sources (crustacean shell waste), an environmentally friendly material of low cost, instead of derived from petroleum based materials. Nevertheless, there are also disadvantages in the use of chitosan or chitosan derivatives. Some of them are the fact that chitosan in flakes or powder is a crystallized polymer, so adsorption takes place in the amorphous region of the crystals, limiting the adsorption capacity. Chitosan beads have reduced crystallinity but they are soluble in acidic media. In the other hand, crosslinked chitosan derivatives, generally insoluble in acidic and alkaline solutions, show a decrease in the fluoride adsorption capacity as amino functional groups involved in crosslinking are not available for ionic exchange with fluoride ions.

Despite the fact that chitosan composites show good performance, more studies are needed to transfer the process to industrial scale. Also, regeneration studies need to be performed in more extent to recover the adsorbent, enhancing the economic feasibility of the process.

The versatility in possible chitosan derivatives let us predict that the F^- sorption performance (equilibrium uptake and removal kinetics) and also the selectivity towards F^- ions can be yet enhanced.

References

[1] WHO, Guidelines for Drinking Water Quality, vol. 1, World Health Organization, 2006 (first addendum third ed.).
[2] F. Diaz-Barriga, A. Navarro-Quizada, M. Grijalva, M. Grimaldo, J.P. Loyola-Rodriguez, M.D. Ortiz, Fluoride 30 (1997) 233–239.
[3] P.L. Smedley, H.B. Nicolli, D.M.J. Macdonald, A.J. Barros, O. Tullio, Appl. Geochem. 17 (2002) 259–284.
[4] S. Ayoob, A.K. Gupta, Crit. Rev. Environ. Sci. Technol. 36 (2006) 433–487.
[5] G. Lee, C. Chen, S.T. Yang, W.S. Ahn, Micropor. Mesopor. Mater. 127 (2010) 152–156.
[6] S. Ayoob, A.K. Gupta, V.T. Bhat, Crit. Rev. Environ. Sci. Technol. 38 (2008) 401–470.
[7] M. Mohapatra, S. Anand, B.K. Mishra, D.E. Giles, P. Singh, J. Environ. Manage. 91 (2009) 67–77.
[8] S. Ghorai, K.K. Pant, Chem. Eng. J. 98 (2004) 165–173.
[9] S. Ghorai, K.K. Pant, Sep. Purif. Technol. 42 (2005) 265–271.
[10] A.L. Valdivieso, J.L.R. Bahena, S. Song, R.H. Urbina, J. Colloid Interface Sci. 298 (2006) 1–5.
[11] N. Das, P. Pattanaik, R. Das, J. Colloid Interface Sci. 292 (2005) 1–10.
[12] S. Meenakshi, N. Viswanathan, J. Colloid Interface Sci. 308 (2007) 438–450.
[13] S. Maliyekkal, A. Sharma, L. Philip, Water Res. 40 (2006) 3497–3506.
[14] Y.H. Li, S. Wang, X. Zhang, J. Wei, C. Xu, Z. Luan, D. Wu, Mater. Res. Bull. 38 (2003) 469–476.
[15] Y.H. Li, S. Wang, X. Zhang, J. Wei, C. Xu, Z. Luan, D. Wu, B. Wei, Environ. Technol. 24 (2003) 391–398.
[16] N.A. Medellin-Castillo, R. Leyva-Ramos, R. Ocampo-Perez, R.F.G. de la Cruz, A. Aragon-Pina, J.M. Martinez-Rosales, R.M. Guerrero-Coronado, L. Fuentes-Rubio, Ind. Eng. Chem. Res. 46 (2007) 9205–9212.
[17] L. Lv, J. He, M. Wei, D.G. Evans, Z.L. Zhou, Water Res. 41 (2007) 1534–1542.
[18] S. Meenakshi, C.S. Sundaram, R. Sukumar, J. Hazard. Mater. 153 (2008) 164–172.
[19] H. Liu, S. Deng, Z. Li, G. Yu, J. Huang, J. Hazard. Mater. 179 (2010) 424–430.
[20] X. Fan, D.J. Parker, M.D. Smith, Water Res. 37 (2003) 4929–4937.
[21] R.C.W. Berkeley, in: R.C.W. Berkeley, C.W. Gooday, D.C. Elwood (Eds.), Microbial Polysaccharides, Academic Press, New York, 1979, pp. 205–236.
[22] M. Zhang, A. Haga, H. Sekiguchi, S. Hirano, Int. J. Biol. Macromol. 27 (2000) 99–105.
[23] J. Synowiecki, N.A. Al-Khateeb, Crit. Rev. Food Sci. Nutr. 43 (2003) 145–171.
[24] M.N.V.R. Kumar, React. Funct. Polym. 46 (2000) 1–27.
[25] H. Sashiwa, S. Aiba, Prog. Polym. Sci. 29 (2004) 887–908.
[26] A.J. Varma, S.V. Deshpande, J.F. Kennedy, Carbohydr. Polym. 55 (2004) 77–93.
[27] G. Crini, Prog. Polym. Sci. 30 (2005) 38–70.
[28] K. Kurita, Mar. Biotechnol. 8 (2006) 203–226.
[29] K. Jaafari, T. Ruiz, S. Elmaleh, J. Coma, K. Benkhouja, Chem. Eng. J. 99 (2004) 153–160.
[30] S. Chatterjee, S.H. Woo, J. Hazard. Mater. 164 (2009) 1012–1018.
[31] S. Chatterjee, D.S. Lee, M.W. Lee, S.H. Woo, J. Hazard. Mater. 166 (2009) 508–513.
[32] Y. Xie, S. Li, F. Wang, G. Liu, Chem. Eng. J. 156 (2010) 56–63.
[33] A. Bhatnagar, M. Sillanpaa, Adv. Colloid Interface Sci. 152 (2009) 26–38.
[34] N. Li, R. Bai, Sep. Purif. Technol. 42 (2005) 77–93.
[35] E. Guibal, Sep. Purif. Technol. 38 (2004) 43–74.
[36] K. Kurita, T. Sannan, Y. Iwakura, J. Appl. Polymer. Sci. 23 (1979) 511–515.
[37] S. Chaterjee, T. Chaterjee, S.H. Woo, Bioresour. Technol. 101 (2010) 3853–3858.
[38] J. Zhi, Y. Wang, G. Luo, React. Funct. Polym. 65 (2005) 249–257.
[39] S. Haider, S.Y. Park, J. Membr. Sci. 328 (2009) 90–96.
[40] R. Vieira, M. Beppu, Adsorption 11 (2005) 731–736.
[41] J.L. Davila-Rodriguez, V.A. Escobar-Barrios, K. Shirai, J.R. Rangel-Mendez, J. Fluorine Chem. 130 (2009) 718–726.
[42] S.P. Kamble, S. Jagtap, N.K. Labhsetwar, D. Thakare, S. Godfrey, S. Devotta, S.S. Rayalu, Chem. Eng. J. 129 (2007) 173–180.
[43] C.S. Sundaram, N. Viswanathan, S. Meenakshi, Bioresour. Technol. 99 (2008) 8226–8230.
[44] C.S. Sundaram, N. Viswanathan, S. Meenakshi, J. Hazard. Mater. 172 (2009) 147–151.
[45] C.S. Sundaram, N. Viswanathan, S. Meenakshi, J. Hazard. Mater. 163 (2009) 618–624.
[46] S. Jagtap, D. Thakre, S. Wanjari, S. Kamble, N. Labhsetwar, S. Rayalu, J. Colloid Interface Sci. 332 (2009) 280–290.
[47] S.K. Swain, R.K. Dey, M. Islam, R.K. Patel, U. Jha, T. Patnaik, C. Airoldi, Sep. Sci. Technol. 44 (2009) 2096–2116.
[48] D. Thakre, S. Jagtap, A. Bansiwal, N. Labhsetwar, S. Rayalu, J. Fluorine Chem. 13 (2010) 373–377.
[49] D. Thakre, S. Jagtap, N. Sakhare, N. Labhsetwar, S. Meshram, S. Rayalu, Chem. Eng. J. 158 (2010) 315–324.
[50] N. Viswanathan, S. Meenakshi, J. Fluorine Chem. 129 (2008) 503–509.
[51] N. Viswanathan, S. Meenakshi, J. Colloid Interface Sci. 322 (2008) 375–383.
[52] N. Viswanathan, S. Meenakshi, Colloids Surf. B 72 (2009) 88–93.
[53] N. Viswanathan, S. Meenakshi, J. Appl. Polym. Sci. 112 (2009) 1114–1121.
[54] N. Viswanathan, S. Meenakshi, J. Hazard. Mater. 176 (2010) 459–465.
[55] N. Viswanathan, S. Meenakshi, Appl. Clay Sci. 48 (2010) 607–611.
[56] N. Viswanathan, S. Meenakshi, J. Hazard. Mater. 178 (2010) 226–232.
[57] P. Sorlier, A. Denuzière, C. Viton, A. Domard, Biomacromolecules 2 (2001) 765–772.
[58] T. Yui, K. Imada, K. Okuyama, Y. Obata, K. Suzuki, K. Ogawa, Macromolecules 27 (1994) 7601–7605.
[59] M. Rinaudo, Macromol. Symp. 245/246 (2006) 549–557.
[60] E. Guibal, Prog. Polym. Sci. 30 (2005) 71–109.
[61] B. Krajewska, Sep. Purif. Technol. 41 (2005) 305–312.
[62] Y. Kawamura, H. Yoshida, S. Asai, Sep. Sci. Technol. 32 (1997) 1959–1974.
[63] K.C. Gupta, M.N.V.R. Kumar, Pure Appl. Chem. A 36 (1999) 827–841.
[64] V.K. Mourya, N.N. Inamdar, React. Funct. Polym. 68 (2008) 1013–1051.
[65] T.-Y. Hsien, G.L. Rorrer, Sep. Sci. Technol. 30 (1995) 2455–2475.
[66] A. Bansiwal, D. Thakre, N. Labhshetwar, S. Meshram, S. Rayalu, Colloids Surf. B 74 (2009) 216–224.
[67] N. Viswanathan, C.S. Sundaram, S. Meenakshi, Colloids Surf. B 68 (2009) 48–54.
[68] N. Viswanathan, C.S. Sundaram, S. Meenakshi, J. Hazard. Mater. 161 (2009) 423–430.
[69] N. Viswanathan, C.S. Sundaram, S. Meenakshi, J. Hazard. Mater. 167 (2009) 325–333.
[70] W. Ma, F.Q. Ya, M. Han, R. Wang, J. Hazard. Mater. 143 (2007) 296–302.
[71] E.W. Giesekke, Int. J. Miner. Process. 11 (1983) 19–56.
[72] A.M. Marabini, G. Contini, C. Cozza, Int. J. Miner. Process. 38 (1993) 1–20.
[73] G. Lachenal, Vib. Spectrosc. 9. (1995) 93–100.
[74] Y. Vijaya, A. Krishnaiah, E- J. Chem. 6 (2009) 713–724.
[75] R. Yao, F. Meng, L. Zhang, D. Ma, M. Wang, J. Hazard. Mater. 165 (2009) 454–460.
[76] M.A. Menkouchi Sahli, S. Annouar, M. Tahaikt, M. Mountadar, A. Soufiane, A. Elmidaoui, Desalination 212 (2007) 37–45.
[77] C.S. Sundaram, N. Viswanathan, S. Meenakshi, J. Hazard. Mater. 155 (2008) 206–215.
[78] S. Ayoob, A.K. Gupta, Chem. Eng. J. 133 (2007) 273–281.
[79] S. Dey, S. Goswami, C.U. Ghosh, Water Air Soil Pollut. 158 (2004) 311–323.
[80] S.S. Tripathy, A.M. Raichur, J. Hazard. Mater. 153 (2008) 1043–1051.
[81] V. Sivasankar, T. Ramachandramoorthy, A. Chandramohan, J. Hazard. Mater. 177 (2010) 719–729.
[82] V. Gopal, K.P. Elango, J. Hazard. Mater. 141 (2007) 98–105.
[83] M. Sarkar, A. Banerjee, P.P. Pramanick, A.R. Sarkar, J. Colloid Interface Sci. 302 (2006) 432–441.

[84] Q. Liu, H. Guo, Y. Shan, J. Fluorine Chem. 131 (2010) 635–641.
[85] R.L. Leyva- Ramos, J.O. Turrubiartes, M. Sanchez-Castillo, Carbon 37 (1999) 609–617.
[86] D. Thakre, S. Rayalu, R. Kawade, S. Meshram, J. Subrt, N. Labhsetwar, J. Hazard. Mater. 180 (2010) 122–130.
[87] J.L. Reyes-Bahena, A.R. Cabrera, A.L. Valdivieso, R.H. Urbina, Sep. Sci. Technol. 37 (2002) 1973–1987.
[88] S.A. Wasay, J.M. Haron, S. Tokunaga, Water Environ. Res. 68 (1996) 295–300.
[89] S.P. Kamble, P. Dixit, S.S. Rayalu, N.K. Labhsetwar, Desalination 249 (2009) 687–693.
[90] V.K. Gupta, I. Ali, V.K. Saini, Water Res. 41 (2007) 3307–3316.
[91] M.G. Sujana, R.S. Thakur, S.B. Rao, J. Colloid Interface Sci. 206 (1998) 94–101.
[92] Y. Cengeloglu, E. Kır, M. Ersoz, Sep. Purif. Technol. 28 (2002) 81–86.
[93] C.S. Sundaram, S. Meenakshi, J. Colloid Interface Sci. 333 (2009) 58–62.
[94] A.M. Raichur, J.M. Basu, Sep. Purif. Technol. 24 (2001) 121–127.
[95] E. Tchomgui-Kamga, E. Ngameni, A. Darchen, J. Colloid Interface Sci. 346 (2010) 494–499.
[96] Y. Zhou, C. Yu, Y. Shan, Sep. Purif. Technol. 36 (2004) 89–94.
[97] H.Y. Li, S. Wang, A. Cao, D. Zhao, X. Zhang, C. Xu, Z. Luan, D. Ruan, J. Liang, D. Wu, W. Wei, Chem. Phys. Lett. 350 (2001) 412–416.
[98] X.P. Liao, B. Ishi, Environ. Sci. Technol. 39 (2005) 4628–4632.
[99] S.M. Onyango, Y. Kojima, O. Aoyi, C.E. Bernardo, H. Matsuda, J. Colloid Interface Sci. 279 (2004) 341–350.
[100] Y.M. Xu, A.R. Ning, J. Zhao, J. Colloid Interface Sci. 235 (2001) 66–69.
[101] X. Wu, Y. Zhang, X. Dou, M. Yang, Chemosphere 69 (2007) 1758–1764.